The development of a novel model of direct fracture healing in the rat

BJR

TRAUMA

The development of a novel model of direct fracture healing in the rat

T. Savaridas,
R. J. Wallace,
A. Y. Muir,
D. M. Salter,
A. H. R. W. Simpson

From the Department of Orthopaedics, The University of Edinburgh, Edinburgh, United Kingdom

T. Savaridas, MBChB, MRCS, MD, Specialty Trainee in Trauma & Orthopaedics
Northern Deanery Orthopaedic Training Programme, Waterfront 4, Goldcrest Way, Newburn Riverside, Newcastle Upon Tyne NE15 8NY, UK.

R. J. Wallace, BEng, MSc, PhD, Postdoctoral Research Associate
A. H. R. W. Simpson, DM(Oxon), FRCS(Eng & Ed), MA(Cantab), Professor of Orthopaedics & Trauma
The University of Edinburgh, Department of Orthopaedics, The Royal Infirmary of Edinburgh, Little France, Old Dalkeith Road, Edinburgh EH16 4SU, UK.

A. Y. Muir, MPhil, C.Phys, M.Inst.P, Co-Director
Edinburgh Orthopaedic Engineering Collaboration, The University of Edinburgh, Chancellor's Building, 49 Little France Crescent, Edinburgh EH16 4SB, UK.

D. M. Salter, MD, Professor of Osteoarticular Pathology
Osteoarticular Research Group, Centre for Molecular Medicine MRC IGMM, The University of Edinburgh, Wilkie Building, Teviot Place, Edinburgh EH8 9AG, UK.

Correspondence should be sent to Mr T. Savaridas; e-mail: tsavaridas@doctors.net.uk

10.1302/2046-3758.111.2000087 $2.00

Bone Joint Res 2012;1:289–96.
Received 23 April 2012; Accepted after revision 4 October 2012

Objectives

Small animal models of fracture repair primarily investigate indirect fracture healing via external callus formation. We present the first described rat model of direct fracture healing.

Methods

A rat tibial osteotomy was created and fixed with compression plating similar to that used in patients. The procedure was evaluated in 15 cadaver rats and then *in vivo* in ten Sprague-Dawley rats. Controls had osteotomies stabilised with a uniaxial external fixator that used the same surgical approach and relied on the same number and diameter of screw holes in bone.

Results

Fracture healing occurred without evidence of external callus on plain radiographs. At six weeks after fracture fixation, the mean stress at failure in a four-point bending test was 24.65 N/mm^2 (SD 6.15). Histology revealed 'cutting-cones' traversing the fracture site. In controls where a uniaxial external fixator was used, bone healing occurred via external callus formation.

Conclusions

A simple, reproducible model of direct fracture healing in rat tibia that mimics clinical practice has been developed for use in future studies of direct fracture healing.

Keywords: Fracture healing, Rat, Model, Bone plates, Equipment design, Tibial fracture/surgery

Article focus

- The rat is increasingly being used as an animal model in fracture healing studies. We describe the development of the first rat model of direct fracture healing

Key messages

- Direct fracture healing is seen to occur in rat diaphyseal bone following compression plate fixation of a transverse tibial osteotomy

Strengths and limitations

- The model of direct fracture healing mimics compression plate fixation
- At six weeks after fixation of the plated osteotomies, the mechanical strength where direct fracture healing occurred was similar to that of the controls that healed with external callus, where an external fixator was applied that used the identical surgical dissection with the same number and size of screw holes in bone to that of the plating model

Introduction

Current models of fracture repair in rodents have only investigated indirect fracture healing via callus formation. Direct fracture healing occurs when fracture fragments are closely approximated and rigidly immobilised.[1,2] Compression of the fracture fragments improves stability of fracture fixation, as it helps to eliminate inter-fragmentary strain. Perren[3] demonstrated that very small amounts of inter-fragmentary strain lead to bridging external callus formation. However, inter-fragmentary strain values of up to 2% enabled direct fracture healing with no bridging external callus to occur in lamellar bone.[3] This is seen in fracture fixation using compression plates. This form of fixation allows early mobilisation and is commonly used to stabilise intra-articular fractures, forearm fractures in the adult, peri-prosthetic fractures, corrective osteotomies and joint fusions.[4]

Direct fracture healing involves new bone formation without the intermediate phase of cartilage deposition. It can be considered to

be an extension of the physiological repair and turnover of bone that is constantly occurring, whereby microfractures are located and removed by osteoclasts.[1,2] New bone is then laid down by the ensuing osteoblasts following in the wake of the osteoclasts. With rigid stability, 'contact-healing' occurs at points of cortical apposition whereby osteonal remodelling units ('cutting-cones') tunnel across the fracture site. 'Gap-healing' occurs in the presence of a minimal fracture gap where newly formed either woven or lamellar bone is deposited parallel to the fracture line within the space between the fracture fragments before remodelling by 'cutting-cones' in the longitudinal weight-bearing axis.[1,5,6]

Following compression plating of transverse osteotomies in the dog radius, Schenk and Willenegger[7] observed primary bone healing with 'cutting-cones' led by osteoclasts traversing cortical bone adjacent to the plate, and gap healing on the far cortex where there was a fracture gap of 0.1 mm. Olerud and Danckwardt-Lilliestrom[6] noted similar findings following compression plating of dog radii and in the less-vascularised dog tibia using the technique described by Schenk and Willenegger.[7] Perren[1] observed the same in rigidly plated sheep fractures. Direct fracture healing has also been observed in the rabbit.[8,9]

It is often stated that bone remodelling does not occur in the rat.[10,11] However, Bentolila et al[12] observed cortical remodelling on confocal microscopy of Fuchsin-stained bone sections near 'microcracks' and resorption associated with osteoclastic tunnelling in adult rat diaphyseal ulna following axial loading. After ten days of loading there were 40% less 'microcracks' compared with the similarly loaded contralateral ulna immediately before death. This suggested that the 'microcracks' were being repaired by a process of bone remodelling. This observation has led us to hypothesise that direct fracture healing would occur in the rat, provided that there was anatomical fracture reduction and a biomechanical environment of absolute stability to permit progression of 'cutting cones' across the fracture site.

A recent review reported that the rat was used in nearly 40% of animal fracture studies published in prominent orthopaedic journals over the last decade.[11] However, a rat model of direct fracture healing has not been previously described. As the processes of direct and indirect fracture healing are radically different, both physical modalities (e.g. ultrasound) and pharmacological agents may have differing effects on the different types of fracture repair. For instance, bisphosphonates that act on osteoclasts may have a profound effect on direct fracture healing but minimal or no effect on indirect fracture healing. Therefore, this model of direct fracture healing was developed to assess the effects of physical and pharmacological agents on direct fracture healing.

Materials and Methods

All animal procedures in this study were approved by the United Kingdom Home Office and adhered to the Animals (Scientific Procedures) Act 1986.

Cadaver and preliminary animal studies. A total of 11 adult ex-breeder male Sprague-Dawley rats (Harlan Laboratories, Blackthorn, United Kingdom) were killed, and the dimensions of the 22 cadaveric tibiae were measured in order to plan the size of the tibial plate for osteotomy fixation. Initial unpublished cadaver trials and preliminary animal experiments using various implant configurations and appropriate refinements in the custom-made jig identified the optimal implant dimensions with which to achieve stable compression plate fixation of a rat transverse diaphyseal tibial osteotomy. Table I details the implants used and the problems encountered at each stage of refinement while developing this model. These final implant dimensions enabled four screws with bicortical hold to be firmly placed in diaphyseal bone and allowed pre-bending[13] of the plate for symmetric compression across the diaphyseal osteotomy site. This plating technique was tested in 15 cadavers.

Animals. A total of 22 skeletally mature ex-breeder male Sprague-Dawley rats (Harlan Laboratories) were used for the *in vivo* testing; they were aged between 11 and 13 months and had a mean weight of 512 g (SD 24.3). Animals were fed standard rat chow and provided with water *ad libitum*. Animals were housed in individual cages at constant temperature (21±1°C) and humidity (45% to 55%) using a 12-hour light/dark cycle.

A total of eight animals were used at the earlier stages of the model development during preliminary animal testing before recognition of the final arrangement for tibial plating (Table I).

A total of ten animals had compression plate fixation of a transverse tibial osteotomy using the final arrangement that was developed as is described here. Of this group, five animals were used for mechanical testing and the remaining five for histology.

In the remaining four animals, a transverse tibial osteotomy was stabilised with a uniaxial external fixator that used the same number and size of screw holes within the rat tibia to that employed in the plating model. Two animals underwent mechanical testing and two were assessed on histology. Animals were killed by induction of terminal anaesthesia at six weeks following surgery.

Surgical procedures. Compression plating . Isofluorane (1% to 3%) inhalational anaesthesia was used. Preoperative antibiotic prophylaxis (1 ml/kg Synulox), fluids (10 ml/kg 0.9% saline) and analgesia (0.05 mg/kg buprenorphine) administered subcutaneously. The right hind leg was infiltrated with 0.4 ml/kg of 1% Xylocaine before skin incision. The anteromedial approach to the tibia was used, exploiting the interval between tibialis anterior and tibialis posterior.[14] A custom-made four-hole jig was applied to the flat medial surface of the tibia

Table I. Implants used at each stage of refinement for development of the rat model of direct fracture healing

	Plate dimensions (mm)	Screws	Osteotomy	Cadavers (n)	Animals (n)	Observation
Initial arrangement	16 × 4 × 1	1.6 mm diameter. Proximal screws in metaphysis	0.5 mm thick saw	10	2	Proximal screw loosening
1st change	16 × 4 × 1	1.4 mm diameter. All screws in diaphysis	0.1 mm thick circular saw	5	2	Fracture at distal screws on radiology at two weeks
2nd change	12 × 3 × 1	1.2 mm diameter	0.1 mm thick circular saw	5	4	Wide gap on far cortex on histology at six weeks
3rd change	Pre-bent 12 × 3 × 0.8	1.2 mm diameter	0.1mm thick circular saw	5	0	Osteotomy displacement. Fracture on screw insertion
4th change	Pre-bent 12 × 3 × 0.6	1.2 mm diameter	0.1 mm thick circular saw	5	0	Osteotomy displacement. Fracture on screw insertion
Final arrangement	Pre-bent 12 × 3 × 0.4	1.2 mm diameter	0.1 mm thick circular saw	15	10	Better symmetric compression. Direct fracture healing

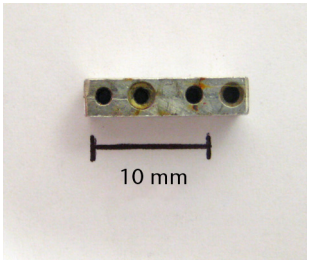

Fig. 1a

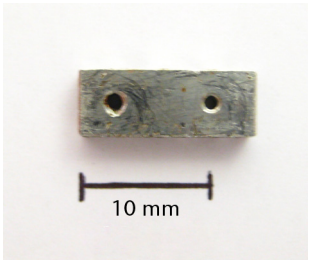

Fig. 1b

Photographs showing the custom-made four-hole jig, showing a) the superior surface, and b) the lateral surface, with two holes used for threading of fine wire to help secure the jig onto bone. There is also a roughened inferior surface (not seen) to prevent the jig slipping on bone during drilling.

(Fig. 1). The spacing between the second and third holes on the jig was 0.1 mm greater (to account for the subsequent osteotomy) than the corresponding holes on the plate, in order to ensure compression at the osteotomy site during plate application. Two holes on the lateral surface of the plate were used to passage a suture to help secure the jig to bone while drilling. Under constant cool saline irrigation, four holes were drilled, with the aid of the jig, using a shortened 1.0 mm drill bit powered by a hand-held Dremel Multitool (Dremel UK, Denham, United Kingdom). The periosteum was stripped circumferentially from the tibia at the level of the osteotomy[8,9] for the length of one diameter of the bone width at the osteotomy site before creation of a transverse tibial osteotomy with a fine circular saw of 0.1 mm thickness (RS Components, Corby, United Kingdom). The osteotomy was aligned manually. Hypodermic needles were placed through the pre-bent (convex)[13] four-hole stainless steel plate (University of Edinburgh Physics Workshop, Edinburgh, United Kingdom), measuring 12 mm × 3 mm × 0.4 mm, into the bone holes to roughly position the plate on the medial surface of the tibia. Four 1.2 mm × 4 mm stainless steel screws (PTS Ltd, East Grinstead, United Kingdom) were used. The screws immediately adjacent to the fracture were inserted first. Then the two more distant holes were filled. Minor adjustments were made with screw tightening to permit plate application on to bone. The two screws adjacent to the fracture were securely tightened earlier than the distant two screws to obtain symmetric compression across the fracture. Then the tibia was manually tested to assess for movement at the fracture site. There was no mobility observed at surgery in any of the animals. 3-0 vicryl (ETHICON; Johnson & Johnson Medical Ltd, Livingston, United Kingdom) was used for wound closure. Post-operatively buprenorphine oral analgesia (0.3 mg/kg B.D) was administered in jelly cubes for 24 hours.

External fixation. The surgical procedure was similar to that of the plate fixation model, except that the 12 mm × 3 mm × 0.4 mm plate was applied as an external fixator on the medial surface of the tibia using longer 1.2 mm × 8 mm stainless steel screws (PTS Ltd). In order to prevent the plate from sliding on the screws, Loctite adhesive (Henkel Ltd, Hemel Hempstead, United Kingdom) was applied to fix the plate to the screw heads. A single interrupted 3-0 vicryl stitch was used to approximate the skin between each screw.

Radiological analysis. Plain anteroposterior (AP) radiographs of the healing fractures were obtained at fortnightly intervals. A portable X-ray unit (Acu-Ray JR; Stern Manufacturing, Toronto, Canada) with an output of 60 kV, 2 mAs and exposure time of 0.1 ms was used. Images were captured on digital X-ray plates (Fuji CR Cassette; Fuji Photo Film Co Ltd, Tokyo, Japan). After death the tibiae were dissected free of soft tissues and the metalwork removed before capture of a standard contact lateral radiograph. Lateral radiographs were obtained to exclude the effect of fibula overlay. The visibility of the osteotomy was observed and scored as totally visible, partly visible, or absent, as previously reported[15,16] by the first author (TS) and an independent assessor (RT) at two separate time points in a blinded manner. Interobserver and intra-observer agreement was assessed using the linear weighted Kappa (κ) test.

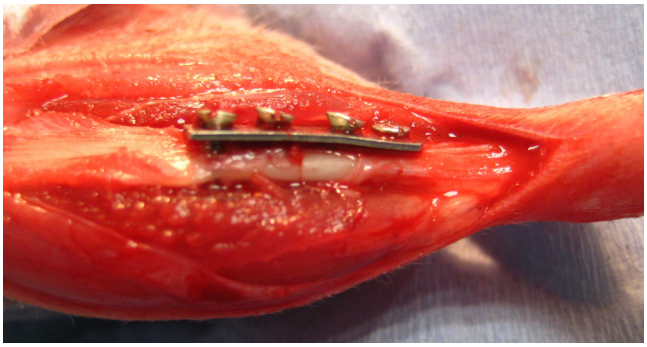

Fig. 2

Intra-operative photograph of tibial plating, showing anatomical alignment and compression at the osteotomy site.

Mechanical testing. The vertical distance from the lateral tibial plateau to the osteotomy site was measured on the injured tibia. A mark corresponding to the location of the tibial osteotomy was made with a pencil on the left contralateral tibia. Extricated tibiae from the uninjured left leg in all animals and from the injured limbs in the seven animals allocated to mechanical testing were placed in individual tubes and frozen at -20°C before mechanical testing within two weeks.[17] Stress test to failure with a four-point bend was performed using a specially designed rig (University of Edinburgh Physics Workshop) in conjunction with a materials testing machine (Zwick/Roell, Ulm, Germany). The upper loading rig was mounted on a pivot in order to ensure symmetrical loading of the irregularly shaped rat tibiae at all four loading points. The upper loading span was spaced 10 mm apart and the lower static span was spaced 20 mm apart. Contact points were rounded to minimise notching of the bone after load application. Specimens were warmed in a water bath set at 37°C for a minimum of 30 minutes before mechanical testing. Immediately, following removal from the water bath tibiae were mounted on the rig resting on the lateral surface. Either, the fracture (operated side) or the pencil mark (un-operated side) was placed at the mid-point between the two lower loading points. The four-point bend was applied while the bone temperature remained at 37°C and well-hydrated. The tibial midshaft cross section following failure most closely resembled a triangle.

The triangular cross section area of the whole bone and intramedullary canal were derived from physical measurements made with sliding callipers and from scaled digital images. This was then used to obtain the cross sectional moment of inertia required to calculate the stress values at failure according to the Euler-Bernoulli Beam Theory, where the peak stress as a result of bending can be approximated by the bending moment multiplied by the distance from the neutral axis to the outermost fibres divided by the second moment of area.[18]

Histological analysis. The remaining extricated tibiae were immersed in 10% formalin in phosphate buffered saline at pH 7.2 to 7.4 for 48 hours, and then decalcified in 10% EDTA at pH 7 and 37°C for four weeks with weekly changes of ethylenediaminetetraacetic acid (EDTA). Three sets of three longitudinal 5 µm coronal sections spaced 100 µm apart were obtained from each specimen and labelled; anterior, middle and posterior. Sections were stained with Masson's trichrome to assess the general morphology at the fracture site. With the aid of a grid, the number of osteoclast on either side of the osteotomy at a distance of 200 µm perpendicular to the line of the osteotomy was manually counted in all sections at × 20 magnification.

Results

All rats were fully weight bearing within 12 hours. There were no post-operative wound complications. One animal in the mechanical testing subgroup of the plate fixation group had an abnormally high force at failure. On inspection of the lateral contact radiograph it was apparent that the posterior cortical hinge was still intact, indicating that the osteotomy had not been completed posteriorly. This animal was excluded from all subsequent analysis.

Cadaver and preliminary animal studies. The measurements of the 22 cadaveric tibiae (11 animals) revealed a mean sagittal width of 3.1 mm (SD 0.2), a mean coronal width of 2.9 mm (SD 0.12) and a mean length of 43.0 mm (SD 1.2). These values corresponded with previously observed tibial dimensions in the adult rat.[19,20] After placing four drill holes in bone with the custom-made jig (Fig. 1) and subsequent transverse tibial osteotomy with a 0.1 mm circular saw, it was observed that a pre-bent 12 mm × 3 mm × 0.4 mm plate secured with four stainless steel screws of 1.2 mm × 4 mm was best suited to achieve stable compression plate fixation (Fig. 2). Of the 15 cadaveric tibial osteotomies that were plated in this manner, none showed movement at the osteotomy site when these constructs were tested with manual bending.

In the initial arrangement (Table I), the osteotomies were created at the proximal diaphysis of the tibia in order to allow the placement of four screws in areas where the tibia remains wide. Unfortunately, as the proximal screws were in metaphyseal bone, they loosened. This was noted on radiographs at five weeks post-operatively. External callus was seen on both histology and radiology. In order to overcome this, the plate was placed more distally on the tibia to allow for all four screws to be in diaphyseal bone. Smaller diameter 1.4 mm screws were used. Furthermore, the integrity of the fibula, despite contributing to stability,[21,22] may have impeded compression at the osteotomy. A narrower osteotomy was therefore created, which could be compressed during plate fixation but remaining in compression despite the effect of the intact fibula in preserving tibial length. These changes were implemented in the first change but between one and two weeks post-fixation the tibia had fractured through the most distal screw holes.

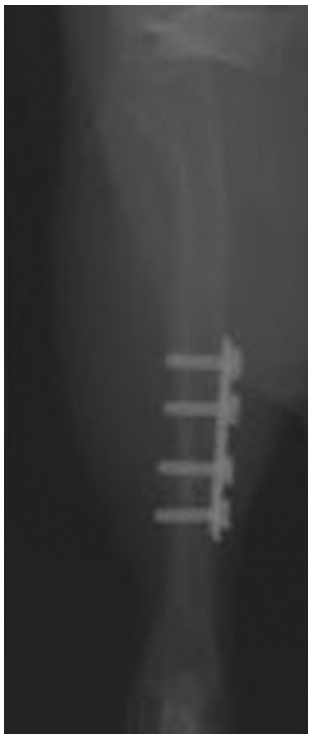

Fig. 3a

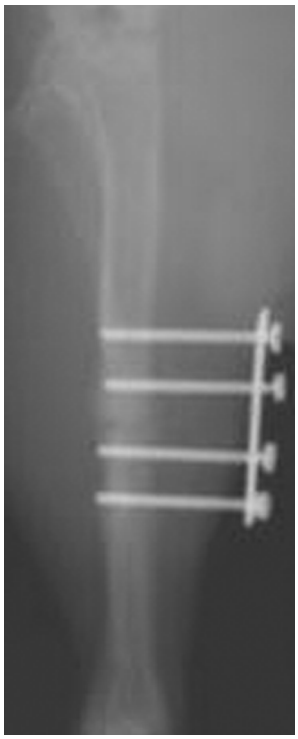

Fig. 3b

Plain radiographs at six weeks after fracture in a) the plate fixation group and b) the external fixation group.

The animals were noted to develop impaired mobility acutely and the fracture was evident on radiographs. Subsequently smaller diameter screws of 1.2 mm were used. The plate width was correspondingly reduced to 3 mm. Serial radiographs revealed no external callus but on histology at six weeks a wide gap was seen on the far cortex away from plate application. After this, plates were pre-bent to permit symmetrical compression across the fracture site.[13] The thicker plates were difficult to pre-bend and occasionally either displaced the fracture or cracked the bone during screw tightening when attempting to conform the plate to the tibial surface in cadaver bone. These problems were not seen in the 15 cadaveric tibiae that were plated with the 0.4 mm plate. This implant was then used for the plate fixation in ten animals, for which the results are presented below.

Compression plating and external fixation: radiological assessment. Test for reliability of the scoring of osteotomy visibility between repeated measurements by the same assessor and between observations by the two separate assessors revealed good intra- and interobserver agreement. There was good intra-observer agreement for both the first author (TS) ($\kappa = 0.77$ (95% confidence interval (CI) 0.48 to 1)) and the independent assessor (RT) ($\kappa = 0.73$ (95% CI 0.42 to 1)). Similarly, interobserver agreement for fracture line visibility between the two observers was good with a κ value of 0.78 (95% CI 0.50 to 1).

Table II. Number of animals based on visibility of fracture line on lateral radiographs following death and metalwork removal

	Absent	Partially visible	Totally visible
Plate fixation			
Author			
First assessment	5	4	0
Second assessment	4	5	0
Independent assessor			
First assessment	5	4	0
Second assessment	6	3	0
External fixation			
Author			
First assessment	0	2	2
Second assessment	0	3	1
Independent assessor			
First assessment	0	3	1
Second assessment	0	4	0

In the compression plating group, serial radiographs at two, four and six weeks post-operatively revealed no visible external callus formation (Fig. 3). At six weeks, in the extricated tibia following plate removal, there was no external callus. On contact radiographs following plate removal there were no animals with totally visible osteotomy lines in the compression plating group (Table II).

In contrast, in the external fixation group serial radiographs after surgery showed fracture healing with external callus formation in all cases. There were no animals with absent osteotomy lines (Table II) on contact radiographs in the external fixation group.

Compression plating and external fixation: mechanical testing. At six weeks the mean load at failure for the direct bone repair (plate fixation) group was 31.0 N (SD 8.5) and the stress at failure was 24.7 N/mm^2 (SD 6.2). The corresponding values for the intact contralateral tibiae were 169.7 N (SD 26.1) and 179.3 N/mm^2 (SD 41.5), respectively. At six weeks in the external fixation group the mean load and stress at failure for the healing tibial osteotomies was 25.9 N (SD 10.6) and 21.8 N/mm^2 (SD 3.0), respectively, and 166.4 N (SD 50.8) and 160.1 N/mm^2 (SD 50.8) for the intact contralateral tibiae, respectively.

Compression plating and external fixation: histology. In all animals in the direct fracture repair group, the Masson's trichrome staining from all three levels confirmed the radiological findings of lack of external callus formation. 'Contact healing' predominated at the medial tibial cortical surface of plate application (5 of 5) and 'gap healing' was seen in the lateral cortex opposite to the plate (5 of 5) (Fig. 4). Osteonal units with leading osteoclasts ('cutting-cones') were seen to traverse the fracture site in all cases indicating direct fracture healing (Fig. 4). When viewed at × 20 magnification, there was a mean of three osteoclasts (2 to 4) seen in each specimen at a distance of 200 μm on either side of the osteotomy.

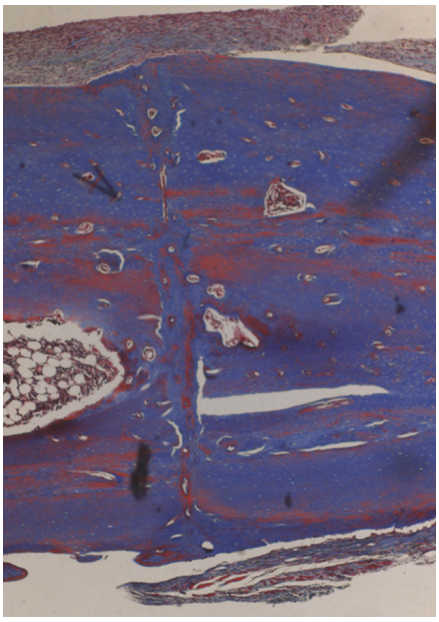

Fig. 4a

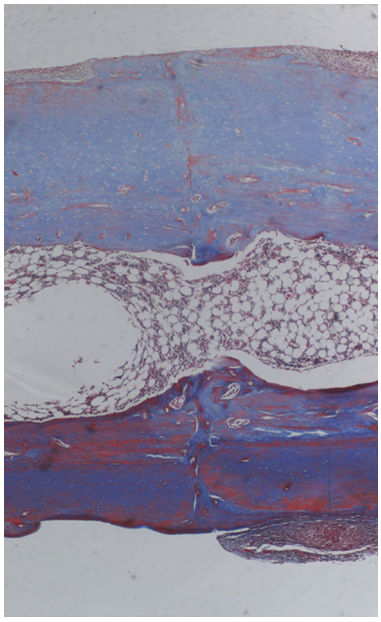

Fig. 4b

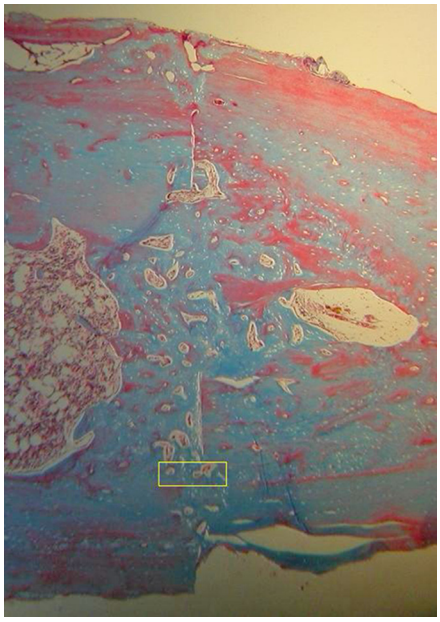

Fig. 4c

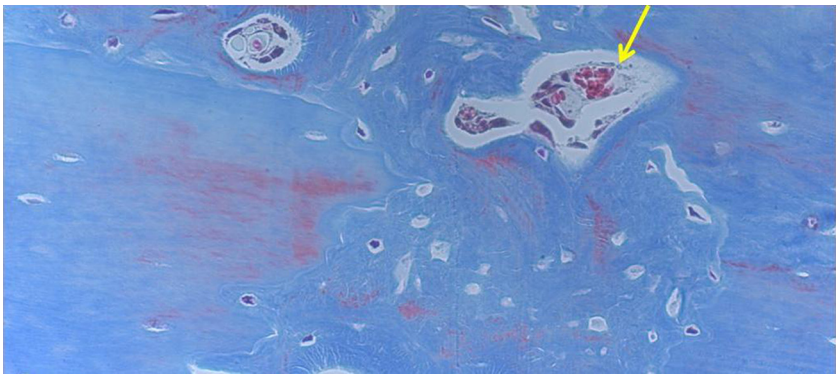

Fig. 4d

Histological images of Masson's trichrome stained sections taken from specimens treated with plate fixation, showing a) the anterior section, b) the middle section and c) the posterior section (yellow box shows area magnified in Figure 4d) (all original magnification ×4). The osteotomy fragments are aligned with no external callus. On the upper aspect note 'contact healing' on the cortical surface of plate application and 'gap healing' on the lower cortex opposite plate application, best seen on middle section (b). Figure 4d – histological image at original magnification ×20, with the arrow showing the 'cutting cone' traversing the fracture site.

In contrast, in all of the animals in the external fixation group, fracture healing occurred with bridging external callus and new woven bone formation (Fig. 5).

Discussion

In this study, a model of direct fracture healing in the rat was developed. A transverse tibial osteotomy was rigidly fixed with compression plating similar to that used in clinical practice for operative fracture management.

The histological appearance of the healing rat tibial osteotomies was similar to that previously reported in the early descriptions of direct fracture healing in the dog,[6,7] sheep[23] and rabbit.[8,9] 'Contact-healing' with 'cutting-cones' traversing the osteotomy predominated at the cortex adjacent to the plate and 'gap-healing' occurred at the far cortical surface with new bone formation observed to be orientated parallel to the osteotomy line.

The use of a small animal model of direct fracture repair is in keeping with the principle of refinement. In addition, there are considerable cost advantages to the size of the animal; the animal cost for the work carried out in this study would have been threefold greater if performed using rabbits. Furthermore, there have been many recent fracture healing studies that have used rat models of indirect fracture healing.[11] The existence of a rat model of direct fracture healing will permit the use of recently developed methods for the study of rat fracture repair to be applied to further investigations that concern direct fracture healing.

Several authors have recently reported models of plate fixation in the femur of rats[24,25] and mice.[26,27] The rat femoral plating models had a 5 mm segmental defect, and were used as models of atrophic nonunion. In both murine plating models,[26,27] fractures healed with less external callus in comparison with controls with less rigid fixation techniques. Post-operative radiographs in these two models also showed an osteotomy gap, suggesting insufficient inter-fragmentary compression. Histing et al[26]

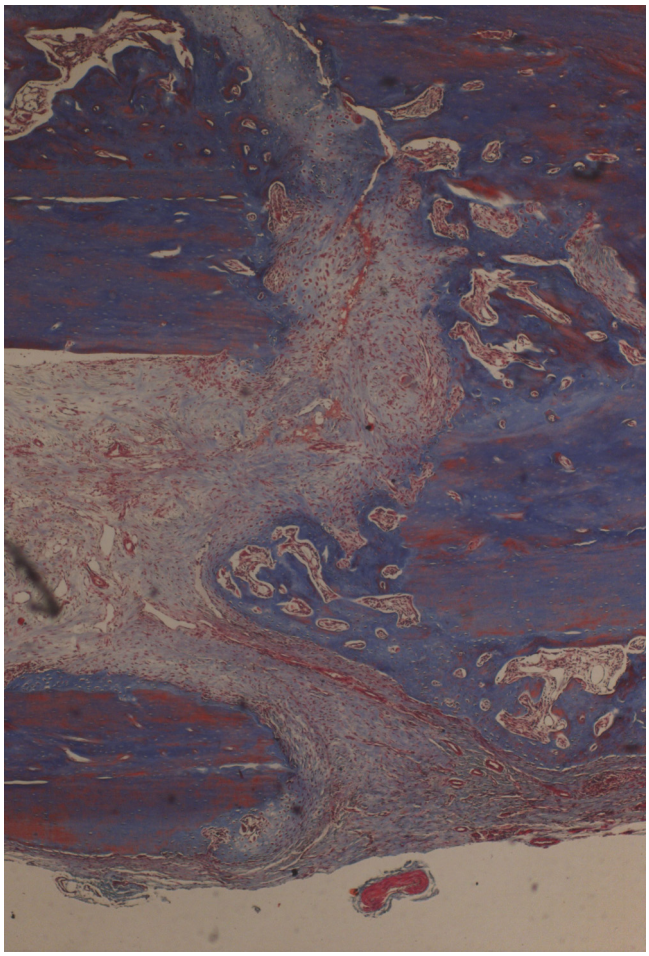

Fig. 5

Histological images of Masson's trichrome ×4 magnification in a specimen of external fixation. Note rim of external callus and new woven bone formation.

reported that their locking plate fixation model of a femoral osteotomy achieved earlier radiological healing and greater fracture stiffness with a non-destructive bending test, in comparison with less rigid fixation with an intramedullary device seen in controls. In the plate fixation group, some callus was observed and no osteonal remodelling units ('cutting-cones') were identified that traverse the fracture site. The authors consider their model to represent intramembranous bone formation rather than direct fracture repair,[26] indeed it is not known whether direct fracture healing will occur in mice. They also noted surgical failure in 20% of their animals (four of 20), described as implant dislocation during fixation.

The model reported in this study reliably produced healing without callus. In this study the length of periosteum for only one diameter of the bone width at the osteotomy was stripped on either side of the osteotomy. This was to prevent excessive disruption to the periosteal blood supply and is less than the periosteal stripping of twice the diameter of bone that was performed by Rahn et al[9] and Ashhurst et al[8] in the previously described model of direct fracture healing in the rabbit. However, in one animal in this study the posterior cortex was not fractured. There is a broad attachment of the deep posterior compartment muscles to the posterior tibia and this area is difficult to visualise. Therefore, care should be taken to ensure the periosteum posteriorly is stripped adjacent to the osteotomy and that the posterior tibial cortex is fractured.

Indirect fracture healing via callus formation in the long bone of an adult rat has been reported to take up to 12 weeks before the restoration of mechanical properties similar to the uninjured side.[28] The process of direct fracture healing proceeds to completion through a lengthier time course.[2,29] The mechanical properties of the fractured bone are not similar to that of the uninjured bone until remodelling is complete. In a plated bone the stresses are transmitted predominantly through the plate initially, protecting the fracture reduction and decreasing load through the fracture. Therefore, at six weeks after fracture fixation, the strength of the rigidly fixed healing tibial osteotomies would not be expected to be similar to that of the contralateral limb. At the six week stage the mean load to failure of the plated rat tibial osteotomies (31.0 N) was slightly greater than in our external fixator group (25.93 N) and the mean value of 27.5 N previously reported in a model of non-rigidly fixed healing rat tibial osteotomies.[15] The values for stress at failure, at six weeks after fracture, in both of our fixation groups, were similar to that obtained by Bak and Andreassen[30] via three-point bending in their rat tibial fracture model that healed with external callus formation. At six weeks Bak and Andreassen[30] noted a mean proportional strength of 12.2% for their healing fractures compared with the contralateral tibia. The mean proportional strength of the healing rat tibial osteotomies within the plate fixation group, in this study was 13.8%.

In summary, we report that direct fracture healing occurs in rat diaphyseal bone. We have developed a reproducible rodent model of direct fracture repair, which may be used in future studies of primary bone healing.

The authors would like to thank Rahul Tyagi MRCSEd, MChOrth for providing radiological assessment of osteotomy healing.

References

1. **Perren SM.** Physical and biological aspects of fracture healing with special reference to internal fixation. *Clin Orthop Relat Res* 1979;138:175–196.
2. **McKibbin B.** The biology of fracture healing in long bones. *J Bone Joint Surg [Br]* 1978;60-B:150–162.
3. **Perren SM.** Evolution of the internal fixation of long bone fractures: the scientific basis of biological internal fixation: choosing a new balance between stability and biology. *J Bone Joint Surg [Br]* 2002;84-B:1093–1110.
4. **Solomon L, Warwick D, Nayagam S.** *Apley's system of orthopaedics and fractures.* 9th ed. London: Hodder Arnold, 2010:311–315,700–703.
5. **Shapiro F.** Cortical bone repair: the relationship of the lacunar-canalicular system and intercellular gap junctions to the repair process. *J Bone Joint Surg [Am]* 1988;70-A:1067–1081.
6. **Olerud S, Danckwardt-Lilliestrom G.** Fracture healing in compression osteosynthesis in the dog. *J Bone Joint Surg [Br]* 1968;50-B:844–851.

7. **Schenk R, Willenegger H.** On the histology of primary bone healing. *Langenbecks Arch Klin Chir Ver Dtsch Z Chir* 1964;308:440–452 (in German).
8. **Ashhurst DE, Hogg J, Perren SM.** A method for making reproducible experimental fractures of the rabbit tibia. *Injury* 1982;14:236–242.
9. **Rahn BA, Gallinaro P, Baltensperger A, Perren SM.** Primary bone healing: an experimental study in the rabbit. *J Bone Joint Surg [Am]* 1971;53-A:783–786.
10. **Nunamaker DM.** Experimental models of fracture repair. *Clin Orthop Relat Res* 1998;355(Suppl):S56–S65.
11. **O'Loughlin PF, Morr S, Bogunovic L, et al.** Selection and development of preclinical models in fracture-healing research. *J Bone Joint Surg [Am]* 2008;90-A(Suppl):79–84.
12. **Bentolila V, Boyce TM, Fyhrie DP, et al.** Intracortical remodeling in adult rat long bones after fatigue loading. *Bone* 1998;23:275–281.
13. **Nunamaker DM, Perren SM.** A radiological and histological analysis of fracture healing using prebending of compression plates. *Clin Orthop Relat Res* 1979;138:167–174.
14. **Greene EC.** Anatomy of the rat. *Trans American Philosophical Society* 1959;27:56–83.
15. **Koivukangas A, Tuukkanen J, Kippo K, et al.** Long-term administration of clodronate does not prevent fracture healing in rats. *Clin Orthop Relat Res* 2003;408:268–278.
16. **Blokhuis TJ, de Bruine JH, Bramer JA, et al.** The reliability of plain radiography in experimental fracture healing. *Skeletal Radiol* 2001;30:151–156.
17. **Sedlin ED, Hirsch C.** Factors affecting the determination of the physical properties of femoral cortical bone. *Acta Orthop Scand* 1966;37:29–48.
18. **Young WC.** *Roark's formulas for stress and strain.* Sixth ed. New York: McGraw-Hill, 1989.
19. **Hornby SB, Evans GP, Hornby SL, et al.** Long-term zoledronic acid treatment increases bone structure and mechanical strength of long bones of ovariectomized adult rats. *Calcif Tissue Int* 2003;72:519–527.
20. **Baumbach B, Sharkey N, Korzick D.** The effects of endurance exercise on the size and strength of adult and aged rat femora and tibiae. Procs American Society of Mechanical Engineers, Sonesta Beach Resort, Florida, 2003.
21. **Horn J, Steen H, Reikeras O.** Role of the fibula in lower leg fractures: an in vivo investigation in rats. *J Orthop Res* 2008;26:1027–1031.
22. **Shefelbine SJ, Augat P, Claes L, Beck A.** Intact fibula improves fracture healing in a rat tibia osteotomy model. *J Orthop Res* 2005;23:489–493.
23. **Perren SM, Huggler A, Russenberger M, et al.** The reaction of cortical bone to compression. *Acta Orthop Scand Suppl* 1969;125:19–29.
24. **Russell G, Tucci M, Conflitti J, et al.** Characterization of a femoral segmental non-union model in laboratory rats: report of a novel surgical technique. *J Invest Surg* 2007;20:249–255.
25. **Mehta M, Schell H, Schwarz C, et al.** A 5-mm femoral defect in female but not in male rats leads to a reproducible atrophic non-union model. *Arch Orthop Trauma Surg* 2011;131:121–129.
26. **Histing T, Garcia P, Matthys R, et al.** An internal locking plate to study intramembranous bone healing in a mouse femur fracture model. *J Orthop Res* 2010;28:397–402.
27. **Ueno M, Urabe K, Naruse K, et al.** Influence of internal fixator stiffness on murine fracture healing: two types of fracture healing lead to two distinct cellular events and FGF-2 expressions. *Exp Anim* 2011;60:79–87.
28. **Ekeland A, Engesoeter LB, Langeland N.** Influence of age on mechanical properties of healing fractures and intact bones in rats. *Acta Orthop Scand* 1982;53:527–534.
29. **Shapiro F.** Bone development and its relation to fracture repair: the role of mesenchymal osteoblasts and surface osteoblasts. *Eur Cell Mater* 2008;15:53–76.
30. **Bak B, Andreassen TT.** The effect of aging on fracture healing in the rat. *Calcif Tissue Int* 1989;45:292–297.

Funding statement:

- Funding for the study was received from the Osteosynthesis & Trauma Care Foundation (AIOD) and the Royal College of Surgeons, Edinburgh

Author contributions:

- T. Savaridas: Developed animal models, performed surgery, data collection and analysis, prepared manuscript
- R. J. Wallace: Data collection and analysis
- A. Y. Muir: Refined materials for models
- D. M. Salter: Data analysis
- A. H. R. W. Simpson: Data analysis, critical revision, manuscript preparation

ICMJE Conflict of Interest:

- None declared